

## Ship wakes and their potential shoreline impact in Tampa Bay

Steven D. Meyers <sup>a,\*</sup>, Mark E. Luther <sup>a</sup>, Stephanie Ringuet <sup>b</sup>, Gary Raulerson <sup>c</sup>, Ed Sherwood <sup>c</sup>, Katie Conrad <sup>d</sup>, Gianfranco Basili <sup>d</sup>

<sup>a</sup> Center for Maritime and Port Studies, Univ. South Florida, 140 7th Av. South, St. Petersburg, FL, USA

<sup>b</sup> City of St. Petersburg, 175 Fifth St. North, St. Petersburg, FL, USA

<sup>c</sup> Tampa Bay Estuary Program, 263 13th Ave South Suite 350, St. Petersburg, FL, USA

<sup>d</sup> US Fish and Wildlife Service, 7915, Baymeadows Way Suite 200, Jacksonville, FL, USA



### ARTICLE INFO

**Keywords:**  
Ship wakes  
Coastal erosion  
Maritime  
Estuary  
Automatic identification system

### ABSTRACT

Ship wakes generated by vessels moving through ecologically sensitive areas, or near poorly-protected infrastructure, can negatively impact these systems. This is especially true in regions hosting large seaports. Ship wakes in Tampa Bay, Florida, were calculated during two time periods using vessel movement data reported through the Automatic Identification System (AIS). The first period was for the years 2015–2017 using data from a government database. The second was during part of 2018 obtained by local monitoring. Only vessels operating at low Froude numbers were examined. Wake heights were estimated from each AIS record using an empirical equation and partitioned by functional vessel class. The largest estimated wakes were produced by the Passenger class. Cargo class vessels had the largest number of ships estimated to produce high wakes. Egmont Key, a long-eroding barrier island at the mouth of the Bay, was potentially subjected to the highest number of ship wakes and the highest cumulative wake energy. Differences in vessel representation in the two sets of AIS data yielded different distributions of wake energy by vessel class. Some strategies for managing wake energy are discussed.

### 1. Introduction

In coastal areas, ship wakes can erode shorelines, submerge habitat, and increase water turbidity (Bilkovic et al., 2017; Gabel et al., 2017; Rapaglia et al., 2015), as well as impact coastal structures (Scully et al., 2020) and other vessels (Fenical et al., 2007; Mortensen et al., 2009). Near large ports there can be several thousand vessel transits per year (Scully, 2016), all producing wakes that vary in height and direction according to vessel size, course, and speed. Understanding the source, frequency, magnitude and location of ship wakes is important for management and mitigation of these potential impacts (Macfarlane and Cox, 2007; Parnell and Kofoed-Hansen, 2001).

Deep water wake generation generally depends on the length-based Froude number  $F_L = U(gL)^{-1/2}$  (Froude, 1877; Hager and Castro-Orgaz, 2016; Watson, 2002), where  $L$  and  $U$  are the ship length and speed, respectively, and  $g = 9.8 \text{ m s}^{-2}$  is the gravitational acceleration. For a particular  $L$ , wake amplitude increases with  $U$ , peaking when  $F_L \sim 0.4$ , where  $U$  reaches the “hull speed” (Toby, 1997; Yousefi et al., 2013) equal to the wave speed for waves with wavelength  $\lambda = L$ . Displacement

vessels are restricted to operating at or below hull speed, as their power consumption increases rapidly due to increasing wave drag as  $F_L$  approaches 0.4. Planing and semiplaning vessels are designed to operate above this speed by exploiting lift forces to raise the bow above the water line, reducing draft, drag, and wake energy (Papanikolaou, 2014; Watson, 2002). Boats in (semi)planing mode decrease their wake height as their speed increases above hull speed.

Wakes are typically delimited by a wedged shape whose cusp is attached to the ship with a half-angle  $\alpha$ . Within the wedge is a complex wave field and outside the wedge there is no significant wave energy. William Thomson, later known as Lord Kelvin, demonstrated in deep water that  $\alpha = \arcsin(1/3) \approx 19.47^\circ$  independent of ship speed  $U$  (Kelvin, 1887, 1906) and that maximum wake height forms an essentially straight line along the wake edge that propagates away from the ship line at angle  $\theta = 35.25^\circ$ , referenced to the forward direction of the ship. Havelock (1908) extended the theory to finite water depth  $h$ , finding  $\alpha$  becomes larger than the Kelvin angle when the depth-based Froude number  $F_h = U(gh)^{-1} \gtrsim 0.7$ , increasing rapidly to  $90^\circ$  as  $F_h \rightarrow 1$ .

Significant progress has recently been made to better understand the

\* Corresponding author.

E-mail addresses: [smeyers@usf.edu](mailto:smeyers@usf.edu) (S.D. Meyers), [mluther@usf.edu](mailto:mluther@usf.edu) (M.E. Luther), [stephanie.ringuet@stpete.org](mailto:stephanie.ringuet@stpete.org) (S. Ringuet), [graulerson@tbep.org](mailto:graulerson@tbep.org) (G. Raulerson), [esherwood@tbep.org](mailto:esherwood@tbep.org) (E. Sherwood), [katie.conrad@fws.gov](mailto:katie.conrad@fws.gov) (K. Conrad), [gianfranco\\_basili@fws.gov](mailto:gianfranco_basili@fws.gov) (G. Basili).

effects of finite waterway breadth and depth, and finite vessel size, on  $\alpha$  and on the wake structure inside the wedge. Several authors (Dias, 2014; Fang et al., 2011; Lee and Lee, 2019; Zhu et al., 2015) have presented theoretical arguments and numerical simulations consistent with Havelock (1908) that demonstrate decreasing wedge angle when  $F_h$  increases beyond  $\sim 0.7$ , with the additional finding of decreasing  $\alpha$  for increasing  $F_h > 1$ . Motion with  $F_h = 1$  is denoted critical,  $F_h < 1$  as subcritical, and  $F_h > 1$  as supercritical motion. Hüsing et al. (2000) identified a transition from subcritical to supercritical over the range of  $0.84 < F_h < 1.15$ , depending on vessel conditions and local bathymetry, where the wake is not clearly in either regime. For  $F_h$  in (or higher) than the transition zone, the maximum wake height moves inside the wedge and the straight edge of the Kelvin solution is replaced by complex curved or “feathered” structures (Noblesse et al., 2016; Pethiyagoda et al., 2015).

Rabaud and Moisy (2013) presented a theoretical model that showed  $\alpha$  decreased with  $F_L$  when  $F_L \gtrsim 0.5$ . They also examined 37 optical images of ship wakes in nearshore waters. They found  $\alpha$  mostly consistent with the Kelvin angle for  $F_L$  up to about 0.6, and decreasing for larger  $F_L$ . Dependence on  $F_h$  was less systematic, with  $\alpha$  ranging  $15^\circ\text{--}22^\circ$  for  $F_h$  up to about 0.9, with some instances of  $5^\circ < \alpha < 15^\circ$ . For larger  $F_h$ , all measured  $\alpha$  were in the lower range.

Nonlinear effects in wakes have been found in the form of solitary (nondispersive) wave solutions that propagate ahead of the vessel (Neuman et al., 2001; Soomere, 2006, 2007). Solitons can form for a wide range of  $F_h$ , but are largest when  $F_h > 1$ . Wake solitons are also produced in narrow channels where they can take the form of a deep trough (depression wave), even at moderate  $F_h$  ( $\sim 0.5$ ) when the cross-sectional area of the vessel is a significant fraction of the channel cross-section (Ertekin et al., 1986; Parnell et al., 2015; Tanimoto et al., 2001). In this case wakes can form a bore-type structure that poses particularly high risk of erosion along the shoreline (Rapaglia et al., 2015).

Field studies of wakes typically involve *in-situ* measurement of quantities such as water pressure with a single or small group of sensors. Such programs have tended to focus on a few ships, or were over limited periods of time, and were spatially restricted (Bauer et al., 2002;

Göransson et al., 2014; Parnell et al., 2015). Due to these limitations, they may not capture wakes from multiple vessels hull types, changing vessel movement, or varying proximity to the shoreline across a large coastal region. There are few published studies examining the cumulative wakes on the shorelines of large estuaries generated near busy ports over longer time periods. Numerical simulations of ship wakes have typically examined a limited numbers of vessels in idealized domains (Benzaquen et al., 2014; Zhu et al., 2018) or in more realistic domains over limited time periods (Safty and Marsooli, 2020). However, they have not been widely applied to large quantities of vessels in realistic domains, largely due to their relatively high computational expense.

Empirical algebraic models offer a possible method for overcoming the spatial and temporal limitations of sensor programs and numerical studies as they have relatively low overhead and can be applied to a large number of vessels, but with somewhat diminished accuracy. Such models are generally designed for a limited hydrodynamic range. Sorensen and Weggel (1985) and Weggel and Sorensen (1986) developed an empirical model (SW) for displacement vessels in open water where  $H$  was dependent on  $F_h$ . The SW model was later modified by Kriebel and Seelig (2005), who introduced dependence on a modified  $F_L$ . In the current study, vessel wakes were estimated using the Kriebel and Seelig (2005) model for many vessel types over three years in Tampa Bay, Florida (Fig. 1) to better assess likely sources of significant wake energy and identify shoreline locations where their cumulative energy is relatively high. The results were partitioned by functional vessel class to help organize this large volume of information.

Section 2 describes the Tampa Bay and its ecological significance, the AIS data, their filtering and error handling, and the methodology employed to estimate ship wake and their shoreline impacts. The bulk of the identified vessels were found to have sufficiently small Froude numbers (Fig. 2) and to operate in largely unrestricted waterways, for which the Kriebel and Seelig (2005) formula was developed. The Results in section 3 present the estimated wake heights, their distribution by vessel class, and the number and energy of their arrival at the shoreline. This is followed by Management section discussing options for reducing wake energy, and a final section of Discussion and Conclusions drawn from the study and describing how uncertainties in this analysis and

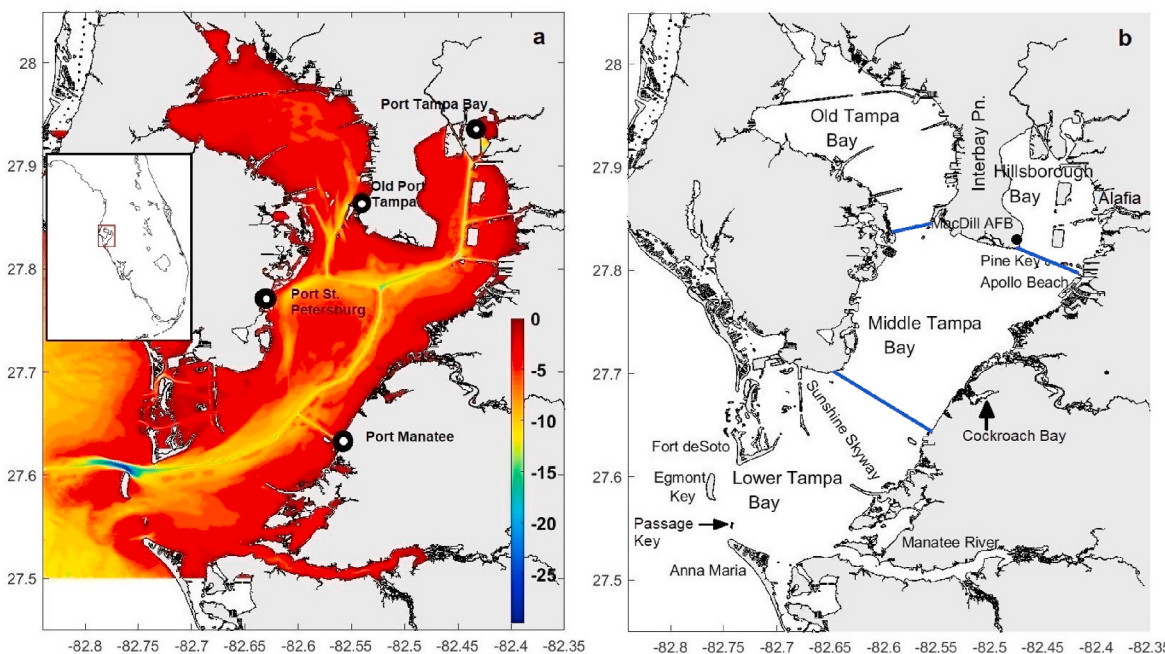


**Fig. 1.** (a) Bathymetry of Tampa Bay with major ports indicated. Location of Tampa Bay on the west coast of Florida, USA (inset). (b) Geographic regions of the bay. Blue lines indicate boundaries between bay sections. (For interpretation of the references to color in this figure legend, the reader is referred to the Web version of this article.)

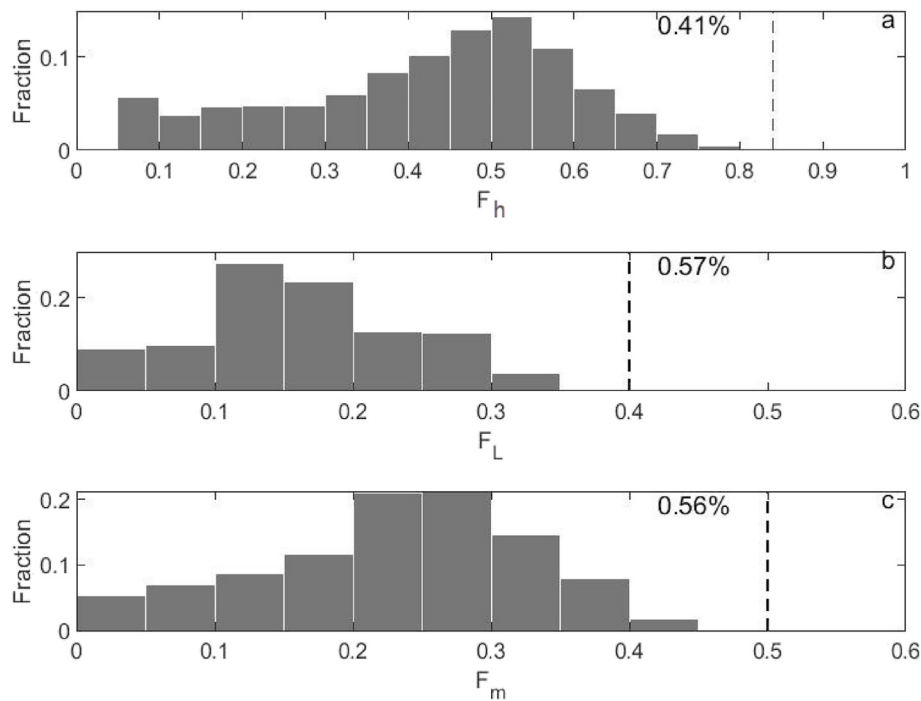


**Fig. 2.** Distribution of Froude numbers calculated from 2015 to 2017 AIS data: a) depth-based, b) length-based, c) modified. Vertical dashed lines are approximate thresholds above which the empirical relation (1) does not apply. The fraction of values from each Froude number above the threshold is indicated.

remaining questions may be addressed.

## 2. Data and methods

### 2.1. Study location

Tampa Bay is an essential sanctuary for water birds, marine life, plants, invertebrates and mammals. Numerous keys and spoil islands in Lower Tampa Bay, Cockroach Bay, and Hillsborough Bay (Fig. 1) have been identified as Important Bird Areas due to the presence of thousands of nesting wading birds, terns, and gulls, and are significant habitat for migrating and wintering shorebirds and migrating neotropical songbirds (Pranty, 2003; Sprandel et al., 2000). Submerged and coastal habitats that are directly impacted by erosion, such as seagrasses, oyster reefs, and mangroves, provide important ecological services (Calil et al., 2015; Chung et al., 2018; Dantis et al., 2020; Menéndez et al., 2018). The bay is connected to the Gulf of Mexico primarily through passes between barrier islands (Evans et al., 1985; Otvos, 1981) located on the southwestern flank of the bay (Fig. 1), between Fort Desoto to the north and Anna Maria Island to the south. This ~8 km passage is partially blocked by Egmont Key, a  $2.8 \times 0.5$  km island whose main axis lies roughly perpendicular to the passage (Berman et al., 2005) and by the smaller Passage Key, both National Wildlife Refuges. Tampa Bay covers about  $1033 \text{ km}^2$ , with a mean depth of 3–4 m and a tidal range of about 1 m (Goodwin, 1987). The primary sections of the bay are: Old Tampa Bay (in the northwest quadrant and spanned by three large bridges), Hillsborough Bay (in the northeast quadrant, containing two large spoil islands), Middle Tampa Bay (whose southern boundary is defined by a line from the Manatee/Hillsborough County line just north of the Sunshine Skyway Bridge), and Lower Tampa Bay (bounded on the west by Egmont Key).

The main shipping channel extends from the mouth north of Egmont Key, into the interior with multiple branches to port facilities (Fig. 1). The main channel has a controlling depth of ~13 m, a nominal width of 200 m (Schoellhamer, 1996; Vincent, 2001), and is generally 3–8 km from the shore. A few hundred large ( $L > 30$  m) vessels make a total of several thousand individual transits (6861 transits in 2017) through

Tampa Bay annually (Meyers et al., 2020). Wake heights from these vessels were estimated using data from records of vessel activity from the Automatic Identification System (AIS), and then propagated to the shoreline. The number of wake impacts and their cumulative energy along the coastline were computed.

### 2.2. The Automatic Identification System

The AIS is a maritime navigation safety communications system, standardized by the International Telecommunication Union (ITU), that has been adopted by the International Maritime Organization (IMO). The AIS was originally developed in the 1990's to enhance ship-to-ship and ship-to-shore awareness. In recent years, AIS records have been widely used as an information source in maritime research (Svanberg et al., 2019). AIS data have been applied to a wide range of research topics, including vessel-to-vessel collision avoidance, quantifying engine exhaust emissions, managing vessel traffic patterns, and prediction of port arrival times (Lim et al., 2018; Tu et al., 2018; Westerdijk et al., 2019; Zhou et al., 2019). The AIS data utilized in this study, along with their filtering and error handling, were detailed by Meyers et al. (2020) so will only be summarized here.

The AIS data consist of reports of vessel conditions sent via radio or satellite and include vessel type and identification numbers, in-water hull dimensions, navigational status, speed and course over ground, and country of registration. Some quantities (e.g., hull dimensions) are set manually by the ship's crew and others are relayed automatically from instrumentation (e.g., position, course, and speed from the vessel's GPS). The manually-entered values are more likely to contain inaccuracies. Errors found in AIS data included incorrect Maritime Mobile Service Identity (MMSI) numbers, drafts deeper than channel control depth, missing or zero vessel lengths ( $L$ ), draft ( $D$ ), and beam ( $B$ , width), blank or zero vessel types, and greater than realistic operating speeds ( $U$ ). Many of these errors were corrected using AIS values from the same vessel but at different times (different transits). Remaining errors were reduced by searching publicly available vessel databases such as [marinetraffic.com](http://marinetraffic.com) or setting upper bounds ( $U < 40 \text{ m s}^{-1}$ ).

There are about 100 AIS vessel types, with descriptor numbers

ranging from 21 to 99 and 1000–1025. For this study, a more manageable framework was created by grouping vessel types into 10 representative classes (Table 1). Within each type, there can be a range of block coefficients ( $C_b$ , defined in Section 2.3) and hull shape (parameterized as  $\beta$ ). However, these specifics were not available for individual vessels, so a nominal value of  $C_b = 0.6$  was used except for some classes as detailed in Table 1, and  $\beta = 1$  in all classes. Only vessels with  $L > 30$  m,  $D < 15$  m, and  $U > 1$  kn ( $\sim 0.51$  ms $^{-1}$ ) were considered.

AIS records for 2015–2017 were obtained from Marine Cadastre, a partnership between the Office for Coastal Management within the National Oceanic and Atmospheric Administration (NOAA) and the Bureau of Ocean Energy Management (BOEM) which is part of the U.S. Department of the Interior. Marine Cadastre offers one of the most complete non-commercial AIS data archives (Tu et al., 2018) covering US territorial waters organized by Universal Transverse Mercator Zones for each calendar month. Tampa Bay is located within Zone 17 and AIS data from the bay was extracted from the monthly records. US Coast Guard (USCG) and other military and law enforcement vessels are often deleted from the Marine Cadastre database.

Port Tampa Bay and ARES Security Corp. provided an additional 617,125 unfiltered AIS reports from Tampa Bay during two time periods in 2018. These data only contained ship MMSI, position, course, speed, and time of each report. Vessel length, draft, width, and type required for this analysis were taken from the 2015–2017 records or scraped from public databases, as noted above. The first of these time periods of unfiltered AIS data began July 6, 2018 and ended July 11, 2018. The second time period began on August 28, 2018 and ended on September 3, 2018. The data provided extended across Florida, but only data within the domain of Tampa Bay were examined.

### 2.3. Wake analysis

The block coefficient  $C_b = V_{ship}/(LBD)$ , which represents the actual underwater volume of the ship  $V_{ship}$  divided by its “block”, has also been

shown to affect wake structure (Larsson et al., 2014; Papanikolaou, 2014; Watson, 2002). Additional relevant ship design details have been discussed by Bertram and Schneekluth (1998), Rawson and Tupper (2001), and Zhang et al. (2008). The geometry of the waterway can also effect wake development and its interaction with the shoreline (MacFarlane, 2006; Pinkster, 2009).

Kriebel and Seelig (2005) adapted an equation for wake height from Sorensen and Weggel (1985) and Weggel and Sorensen (1986) and, based on tow-tank testing of four different model hull forms (a naval vessel, a cruise liner, a tanker, and a cargo ship) at different relative water depths, developed the relation

$$gHU^{-2} = \beta(F_m - 0.1)^2 \left(\frac{y}{L}\right)^{-1/3} \quad (1)$$

where  $H$  is the wake height,  $y$  is the distance from the shipline,  $F_m = F_L \exp(\alpha D/h)$  is the modified Froude number, with  $\alpha = 2.35(1 - C_b)$ . When  $F_m \leq 0.1$  the vessel does not produce a significant wake. The inverse cubic factor in (1) is due to dispersion (Havelock, 1908, 1914). Equation (1) is only considered applicable to  $F_m < 0.5$  in open water.

Field testing using a vessel with  $L = 31$  m and  $D = 1.8$  m operating in fairly still water of depth 5–7 m found good agreement between (1) and measured wake heights, performing better than the SW model (Kriebel and Seelig, 2005). Other tests of (1) have been limited and produced mixed results. Göransson et al. (2014) measured the maximum wake heights for vessels traveling in a river of width  $\sim 150$  m and maximum depth roughly 6–8 m. They found a fair correlation between the secondary wake and (1) for amplitudes up to about 0.5 m, the limit of their sampling. Mao et al. (2020) compared (1) to maximum trough of depression wakes in part of the Grand Canal, China, a narrow waterway  $\sim 90$  m across and 3.2 m deep. They found poor agreement, though this may have been due to application of (1) to a confined waterway. Scully and MacCartney (2017) did not test (1), but applied it to estimate vessel wake heights from large vessels passing through Charleston Harbor as identified from AIS records. We employed a similar method, using AIS to

**Table 1**

Vessel classes, their color designation, the AIS vessel types comprising each class, their block coefficients ( $C_b$ ) and corresponding references (Barrass and Derrett, 2011; Botha, 2000; McTaggart and Stredulinsky, 2004; Soares, 1993; Teixeira and Soares, 2002). (For interpretation of the references to color in this figure legend, the reader is referred to the Web version of this article.).

<u>Class</u>	<u>AIS Vessel Type</u>	<u><math>C_b</math></u>	<u>Reference</u>
Tanker	80-89, 1017, 1024	0.8	(Soares, 1993; Teixeira and Soares, 2002)
Fishing	30,1001,1002	0.6	
Cargo	70-79,1003,1004, 1016	0.7	(Watson, 2002)
Recreational	36,37,1019	0.4	(Larsson et al., 2014)
Tug	21,22,31,32,52, 1023,1025	0.6	(Botha, 2000)
Supply	1010	0.7	
Enforcement	35,50*,53*,55	0.5	(McTaggart and Stredulinsky, 2004)
Passenger	60-69, 1012-1015	0.6	(Barrass and Derrett, 2011)
Research	1020	0.6	
Other	all others	0.6	

identify vessel characteristics, positions, speed, and course over ground, and utilized (1) to estimate initial wake heights.

Application of the Kriebel and Seelig (2005) algorithm in Tampa Bay was found to be justifiable for the majority of the region and vessel movements. The cross-sectional area of the main channel is  $A_w \sim 1900 \text{ m}^2$ , with an additional  $700 \text{ m}^2$  of essentially open water above. The water between the channel and the shore adds roughly  $10,000\text{--}20,000 \text{ m}^2$  for most of the bay. Even for the largest ships ( $B=30 \text{ m}$ ,  $D = 13 \text{ m}$ ) transiting the bay, the maximum vessel cross section  $A_s = BD$  is relatively small, with a blocking coefficient  $A_s/A_w \sim 0.04$ . Confinement effects are therefore likely to be small, though they cannot be ruled out entirely through this simple argument. There are some channel areas immediately adjacent to ports where the waterway greatly narrows and  $A_s/A_w \sim 0.5$ . Depression wakes can be expected at these locations and were not part of this study.

The Froude numbers calculated using the AIS data indicated over 99% of the 2015–2017 recorded vessel activity were within the range of applicability of the model (Fig. 2). The small number of AIS reports (about 0.5%) with  $F_L \geq 0.4$ ,  $F_m \geq 0.5$ , or  $F_h \geq 0.84$  were removed from the 2015–2017 analysis. About 5% of the 2018 AIS data was similarly removed. In 2015–2017 most of the high Froude number vessels were

found in the Passenger and Recreational classes, and in 2018 Passenger and Enforcement classes contained higher Froude numbers (Fig. 3). Larger ships ( $L > 50 \text{ m}$ ) were operating at low Froude numbers throughout all examined records. Restricting the analysis to small Froude number and assuming limited influence of the coastal boundary suggested the wake structures arising from the recorded vessel traffic and their propagation can be represented by the Kelvin solution. This was taken as a reasonable hypothesis in this study, but one that requires further testing. Having noted this caveat, we proceed with the analysis.

### 3. Results

#### 3.1. Wake heights 2015–2017

Wake heights were estimated for underway vessels based on the 2015–2017 AIS data using (1). About 15% of the records were estimated to have no wake ( $H = 0$ ) and 70% of the estimated wake heights were found to be  $< 0.1 \text{ m}$ . Large wakes were relatively rare. Only 0.8% of all the 2015–2017 records indicated  $H > 0.5 \text{ m}$ . Of these, cargo vessels had the largest number of individual vessels (49 out of 765) moving under conditions estimated to result in large wakes (Fig. 4). However, the fraction of AIS reports from cargo vessels with large  $H$  was relatively small (0.48%).

Passenger vessels had the highest percentage of large estimated  $H$ , occurring 9.6% of the time from 17 out of 24 vessels, and the highest estimated  $H$  of all classes. Recreational vessels (yachts) had the second highest rate of high wake generation (1.1%), though their absolute number (11) was relatively small.

The upper limit of  $H$  for all classes generally increased with vessel length  $L$  (Fig. 5). Large Passenger and Cargo class ships ( $L = 250\text{--}300 \text{ m}$ ) generated the highest estimated  $H$ . For relatively small vessels,  $L \lesssim 50 \text{ m}$ , Tug class vessels were the most common source of large  $H$ , but 2 high speed Passenger ships, 3 personal Recreational vessels, and 1 USCG ship yielded the highest estimated wakes of their size. In contrast, the upper envelope of estimated  $H$  was not consistently dependent on  $D$  (Fig. 5). The largest estimated  $H$  peaked around  $D = 8 \text{ m}$ , the typical draft of the large passenger vessels, and generally declined for  $D \gtrsim 10 \text{ m}$ . The vessels with the highest  $D$ , which were all Cargo and Tanker class vessels, mostly had estimated  $H < 0.4 \text{ m}$ , probably due to their relatively low speed compared to Passenger class ships (Meyers et al., 2020). AIS reports of  $D > 13 \text{ m}$  may be in error.

Instances of Cargo and Passenger class vessels generating high estimated wakes ( $> 0.5 \text{ m}$ ) were found along most of the main shipping channel, from west of Egmont Key to northern Hillsborough Bay (Fig. 6), but were largely absent in Old Tampa Bay. High wakes from Tug class were generally confined to Middle and Lower Tampa Bay, as was the case for Enforcement and Research class vessels. Tanker and Fishing classes typically had the lowest maximum wakes, and the highest wakes from these two classes were found near Egmont Key. There was no large-vessel traffic in Old Tampa Bay north of Old Port Tampa and only moderate wakes ( $< 0.5 \text{ m}$ ) were estimated in its southernmost extent (Fig. 6). The region around Old Port Tampa was estimated to experience no more than  $H = 0.4 \text{ m}$  generated by Tugs, with little wake generation from the other classes. Potential wake generation in Tampa Bay was not exclusively limited to the shipping channels. Recreational vessels, and to a lesser extent Passenger vessels, were estimated to generate large wakes outside the channels.

#### 3.2. Wake heights 2018

Like the 2015–2017 data, most ships sending AIS reports during the few weeks of 2018 appeared to be operating in displacement mode, with  $F_L < 0.4$  (Fig. 3b). The high Froude number reports comprised 4.4% of the data, higher than in the prior data set, and were more unevenly distributed among vessel classes. The Other class initially had a large fraction (70%) of AIS reports indicating  $F_L > 0.4$  and 52% had  $F_h > 0.84$ .

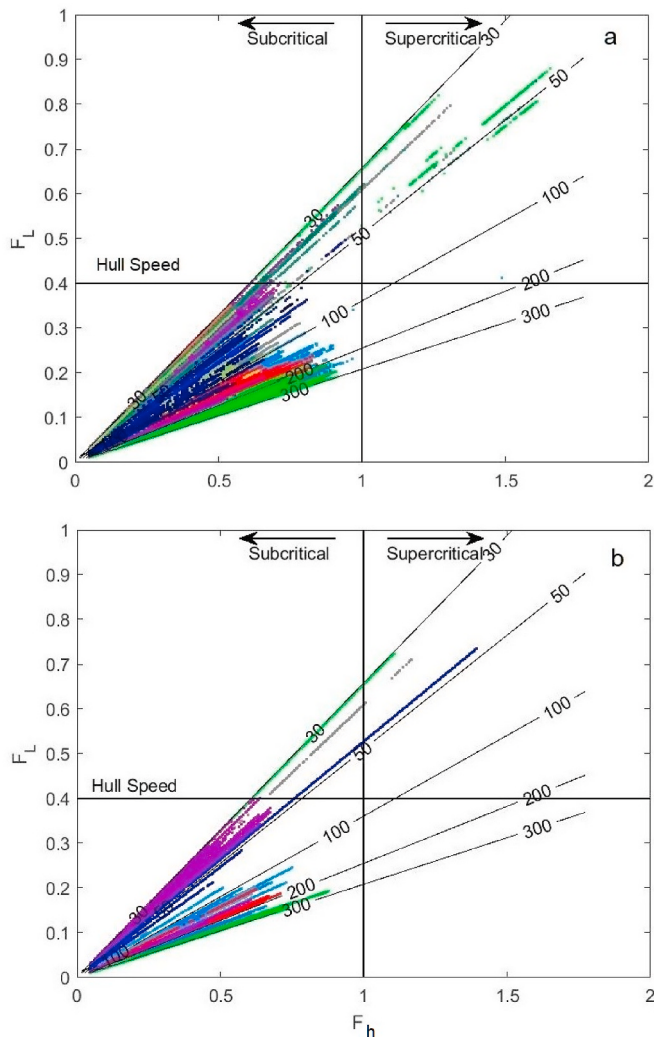


**Fig. 3.** Length-based Froude number ( $F_L$ ) vs. depth-based Froude number ( $F_h$ ), colored by vessel class (Table 1). (a) Based on AIS from 2015 to 2017 Marine Cadastre database; (b) based on AIS from local providers during 2018. The horizontal line is approximate hull speed, vertical line is critical speed, and isolines are ship length in meters.

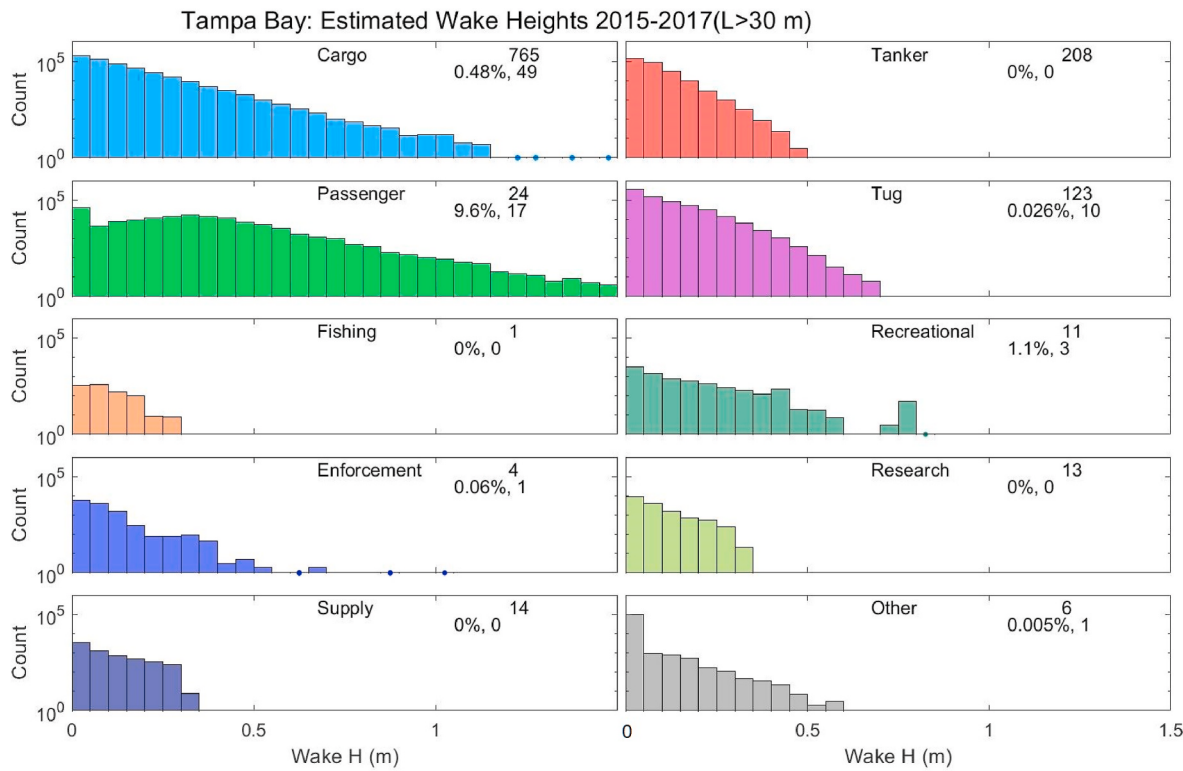


**Fig. 4.** Distributions of estimated wake heights for each vessel class (Table 1). Also indicated are the number of unique vessels within each class, the percentage of AIS reports within each class indicating  $H > 0.5$  m, and the number of unique vessels with  $H > 0.5$  m.

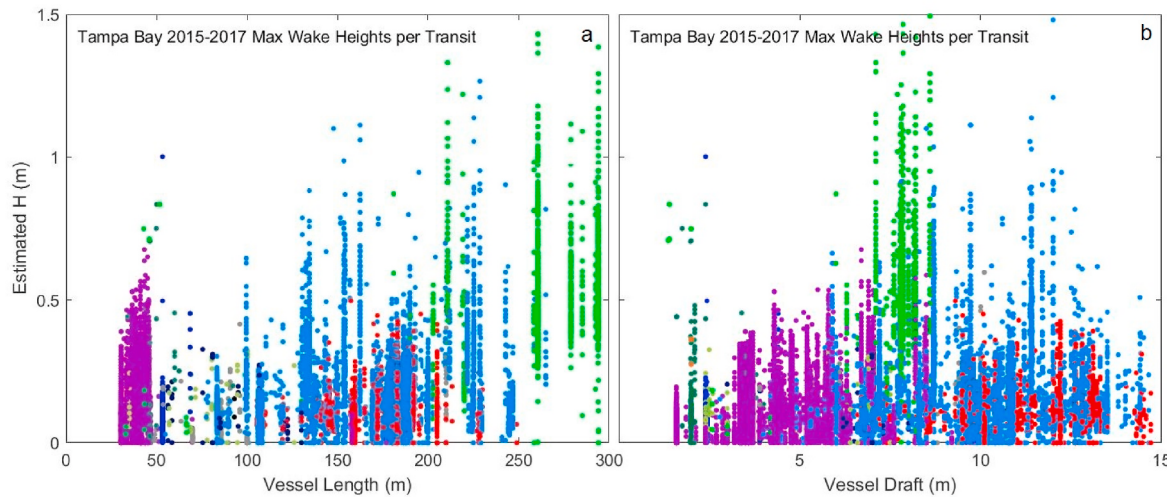


**Fig. 5.** The maximum estimated wake height by (a) vessel length, and (b) vessel draft, for each vessel transit based on 2015–2017 AIS records. Colors indicate vessel class as in Table 1. (For interpretation of the references to color in this figure legend, the reader is referred to the Web version of this article.)

About 20% of Enforcement class AIS reports initially had Froude numbers above these levels from one vessel that was identified from its MMSI as a US Coast Guard Patrol Boat.

In the 2018 data, Passenger class ships were again estimated to generate both the largest and most frequent large  $H$ , with four out of five Passenger vessels estimated to have generated  $H > 0.5$  during about 18% of their operating time (Fig. 7). One of the most significant difference between the estimated wake heights in the two different AIS data sets was in the Enforcement class, which in 2018 had 1 (of 4) vessel generating large  $H$  during 4.1% of the total operating time for this class. The Other class was comprised of two vessels that generated low  $H$ , the majority of this class was removed from the analysis due to high Froude

numbers (Fig. 3). The removed data was from a single ship that was tentatively identified as a US Navy vessel.

### 3.3. Shoreline impacts 2015–2017

Wake propagation away from the ship line occurs at the angle  $\theta = 35.25^\circ$ , referenced to the forward direction of the ship (Rayleigh, 1885). The direction of vessel travel (course over ground,  $\gamma$ ) was extracted from the AIS records. Two wake directions, corresponding to the two sides of the 'V' pattern, were calculated,  $\gamma \pm \theta$ . When the estimated  $H$  was  $> 0$ , both sides of the wake were projected in straight lines at these angles from the AIS point until they hit the Tampa Bay shoreline. The distance

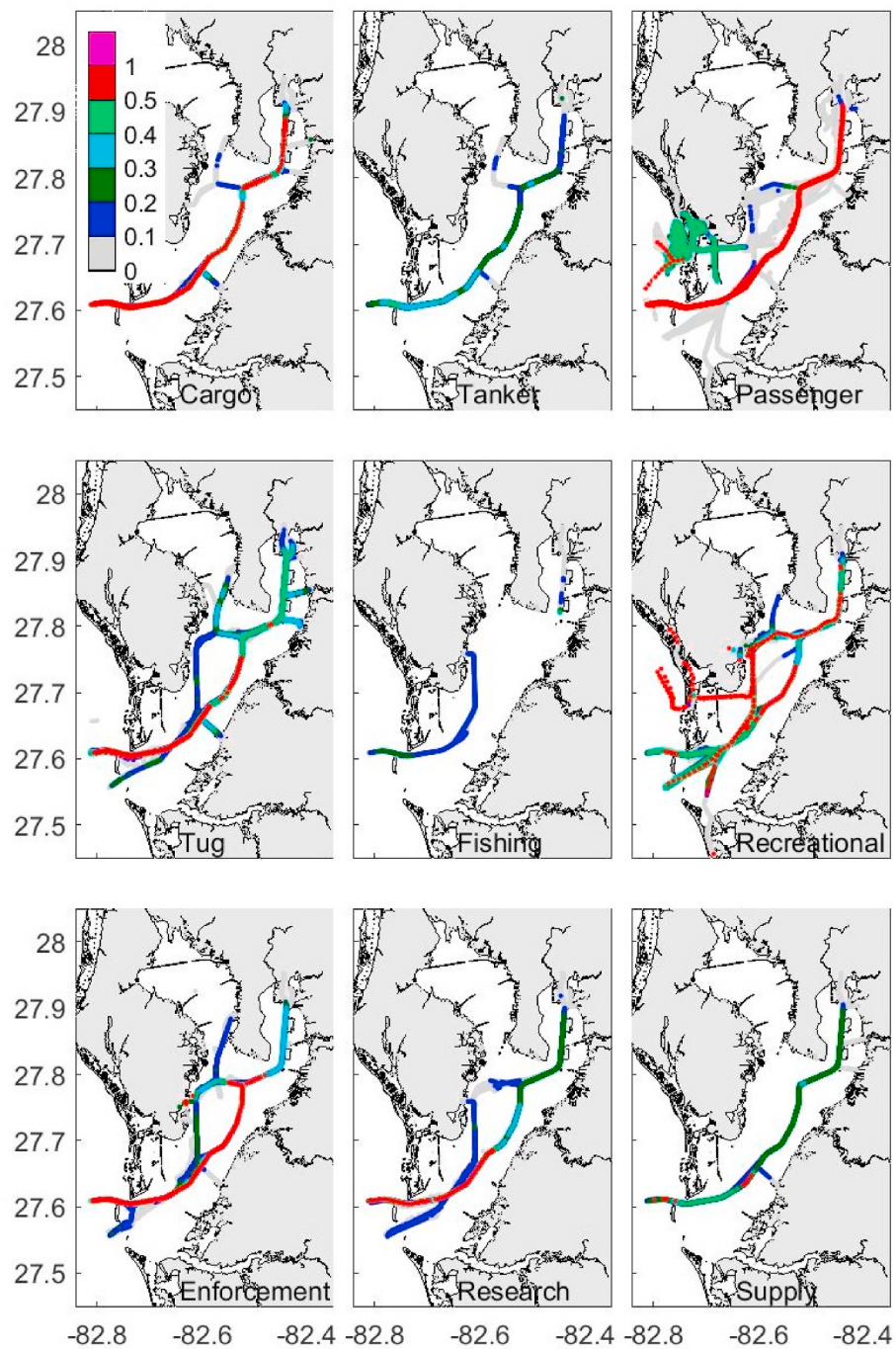


**Fig. 6.** The distribution of wake heights based on the 2015–2017 AIS data by class as indicated. Colors denote maximum wake height at each position. Units are meters. (For interpretation of the references to color in this figure legend, the reader is referred to the Web version of this article.)

from the AIS point to the shoreline was calculated and the wake height at the determined distance from the vessel was estimated using (1).

The shoreline of Tampa Bay was defined using approximately 43,000 spatial points obtained from the NOAA Shoreline Explorer (<https://www.ngs.noaa.gov/CUSP/>). The typical distance between shoreline points was 10–50 m, but there were a few larger gaps up to roughly 100 m. In some instances, wake propagation lines from discrete vessel positions can pass through these gaps. Therefore, the impact of a wake on the shoreline was defined to be the first approach of the wake to the shoreline such that the distance between the wake and shoreline point was  $< d_l$ , which was empirically chosen to be  $d_l = 75$  m, slightly more than half the largest gap in the shoreline data. For each year, the total number of wake impacts on each shoreline point and the total wake

energy were calculated. The calculations were not adjusted for shoaling or other topographic effects as these were beyond the scope of this study.

Regions with a relatively high concentration of potential wake impacts were most often found in the southwestern portion of the bay, particularly along Egmont Key, and on the eastern shoreline (Fig. 8). In all years the point with the largest number of estimated impacts was located on Egmont Key, with over 6000 individual wakes. This number declined from 2015 to 2017, possibly due to changes in vessel operations as the number of vessel transits trended higher over this time period (Meyers et al., 2020). Other regions of potentially high impact were the western side of the spoil islands in Hillsborough Bay, Apollo Beach just south of Hillsborough Bay, and Port Manatee (Fig. 1).

The locations with the largest estimated cumulative wake energy

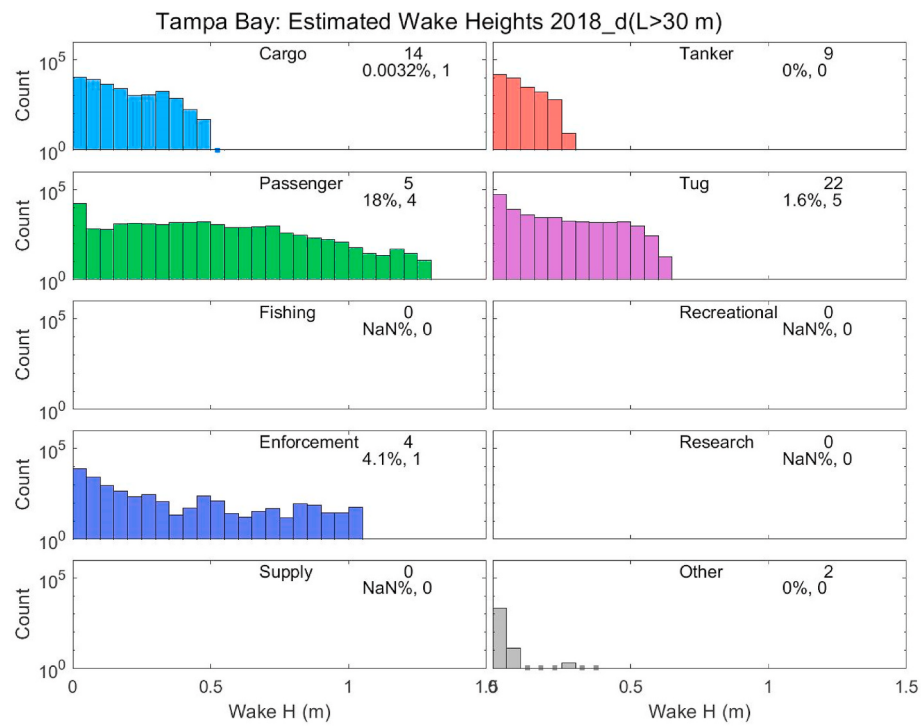


**Fig. 7.** Same as Fig. 4 but based on the 2018 unfiltered AIS data.

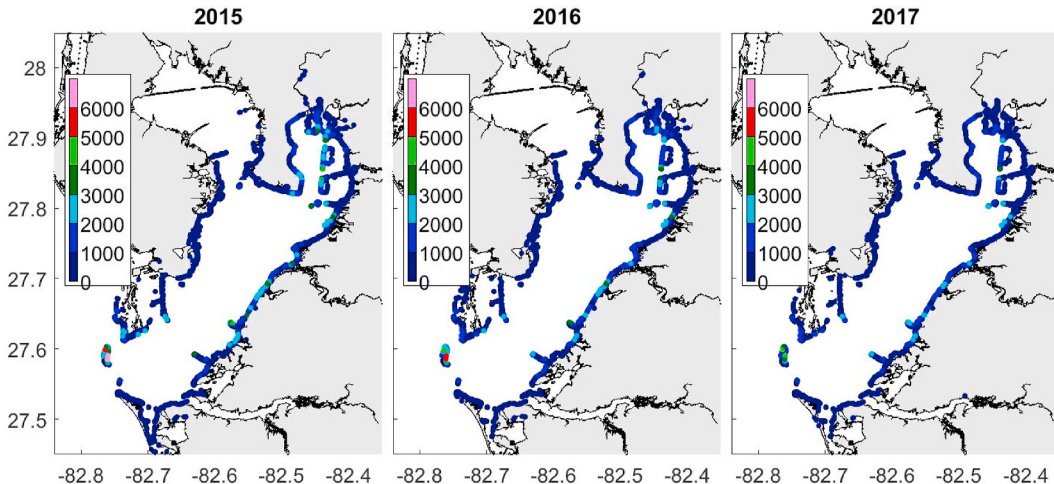


**Fig. 8.** The number of wake impacts estimated from AIS records for the years indicated.

were also on Egmont Key (Fig. 9), largely due to the number of vessels traveling close to the shoreline and their relatively high speeds. Here the total calculated wake energy was  $1\text{--}2 \text{ MJ m}^{-1}$  (Table 2), compared to baywide median values almost three orders of magnitude smaller. The western side of Ft. DeSoto and the tips of the Sunshine Skyway causeways also consistently received high wake energy for similar reasons. Other areas of high energy often corresponded to a high number of wakes, such as the western spoil islands and Apollo Beach. Some regions with a relatively low number of wake impacts were found to have higher than expected wake energies, including the southeastern tip of the interbay peninsula, the entrance to Cockroach Bay, and the northern shore of Anna Maria Island.

#### 4. Management

The relatively low occurrence of high estimated  $H$  and its sensitivity

to vessel speed suggests that with minimal changes in vessel operations within the bay, a significant reduction of potential shoreline impacts due to wakes could be realized. Reducing the reported speeds in the 2015–2017 AIS data by only 1 kn resulted in a decrease in the occurrence of high estimated  $H$  by a factor of  $\sim 2$  for the most common vessel class (Cargo) and by a factor of  $\sim 1.5$  for the Passenger class (Table 3). This reduction in speed would create slightly longer transits through the  $\sim 50 \text{ km}$ -long channel. For example, reducing vessel speed from 20 kn to 19 kn would add about 4 min to the  $\sim 83 \text{ min}$  transit from bay entrance to the northern ports. Changes in transit times would likely have to be accounted for in vessel scheduling. However, as the number of transits estimated to generate high  $H$  was a small percentage of the total traffic, these hypothetical changes would likely have negligible impact on overall port operations.

Even a small speed reduction may not be justified within all sections of the bay, as some shorelines can be reinforced using alternative green

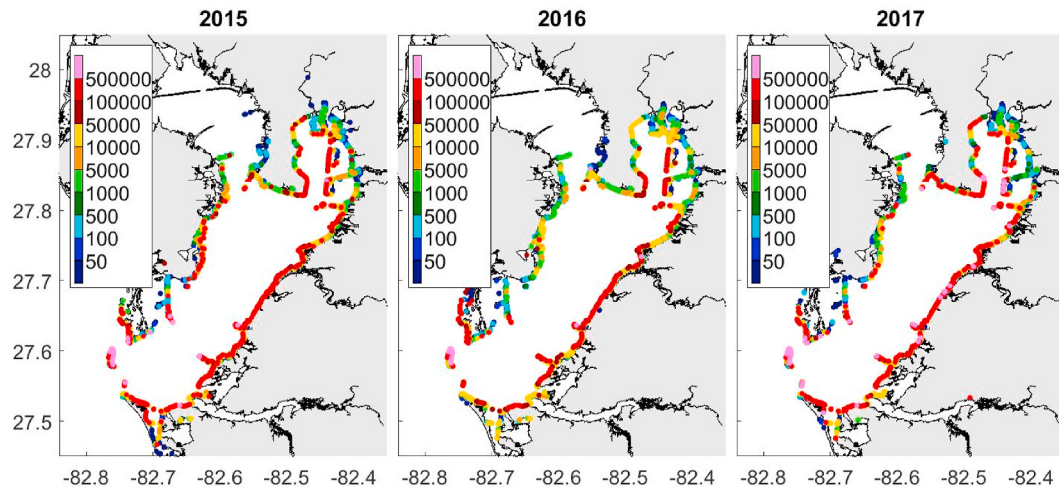


**Fig. 9.** Cumulative wake energy ( $J \text{ m}^{-1}$ ) for the year indicated.

**Table 2**

Statistics of wakes impacting shorelines in Tampa Bay by year. The number of shorelines points with wakes, the average number of wakes impacting these points, the maximum number of wakes impacting these points, the average, median, and maximum energy impacting the points (to three significant digits).

Year	# points	avg #	max #	avg E ( $J \text{ m}^{-1}$ )	median E ( $J \text{ m}^{-1}$ )	max E ( $J \text{ m}^{-1}$ )
2015	2797	281	6707	41500	2620	1630000
2016	2707	243	5550	26100	2100	1260000
2017	2375	201	4806	56200	2580	2080000

**Table 3**

The percentage of estimated  $H > 0.5 \text{ m}$  by vessel class based on 2015–2017 AIS-reported vessel parameters ( $V_0$ ), and with speeds reduced by 1 kn ( $V_0-1$ ).

Class	Occurrence of High $H$	
	$V_0$	$V_0-1$
Cargo	0.48	0.22
Tanker	0	0
Passenger	9.6	6.4
Tug	0.026	0.0011
Fishing	0	0
Recreational	1.1	0
Enforcement	0.6	0.62
Research	0	0
Supply	0	0

shoreline protection. These are broadly categorized as ‘living shorelines’ and have received increasing recognition (Gittman et al., 2014; Herbert et al., 2018). Living shorelines provide wave attenuation, erosion protection, and (in many instances) increased resilience in the form of land accretion that decreases erosional susceptibility. In this sense they function similar to riprap, but with the added value of complementary ecosystem services such as fish nurseries, water quality improvement, and shoreline stabilization (NOAA, 2015).

Currently there are no quantitative speed restrictions in Tampa Bay, only the maritime rule that vessels must operate safely (<https://www.tampabaypilots.com/channels-berths>). Further work on ship wake effects in Tampa Bay should be performed, as discussed below, before any such restriction could ultimately be justified. However, given the rarity of large  $H$ , a navigation advisory or similar guidance may be preferable to enacting stricter regulation.

## 5. Discussion and conclusion

Wakes in Tampa Bay were estimated for ships with  $L > 30 \text{ m}$  over a three year period (2015–2017) using pre-processed AIS data, and over a few weeks in 2018 using unfiltered AIS data. Speed and vessel length were determined to be the most important factors leading to large wakes. Longer vessels with moderate draft were estimated to produce the largest wakes due to their higher speed. The deep draft vessels rarely produced high wakes, probably resulting from their slower transit of the shipping channel because of limited maneuverability, and to reduce vessel “squat”. The relatively small number of Cargo vessels that produced higher wakes may have had lower draft after unloading cargo, allowing for higher speeds. However, the inbound and outbound transits were not examined separately in this study, so this possible change in vessel behavior before and after unloading remains open.

A notable difference was found between the vessels represented in the Marine Cadastre AIS data and the locally provided AIS data: military and some other Enforcement vessels were largely excluded from the former data set. However, the AIS transmissions of these vessels are available locally via most AIS receivers, as was the case in the 2018 data considered here. It is unclear if these vessels are included with third-party commercial data from providers such as GateHouse Maritime or Marine Traffic. Future studies of ship wakes and their effects should seek to fully represent Enforcement vessels.

The length restriction of 30 m helped focus the study on commercial vessels. However, smaller vessels might also produce significant wake energy along the shoreline. These tend to be personal craft and can typically operate much closer to the shore due to their relatively shallow draft, potentially generating wakes tens of meters from the shore, decreasing dispersive effects in (1), and resulting in high  $H$  when the wakes hit the shore. There are many personal craft that do not have an AIS transmitter and cannot be examined using the applied methodology.

The cumulative wake energy in Tampa Bay was found to be irregularly distributed along the shoreline (Fig. 9), mostly due to differences in distance of the shoreline from the shipline, as well as vessel behavior. These variations in energy distribution indicated some regions are potentially subject to higher wake disturbance than others, creating regions of increased erosion around the bay. For example, Egmont Key, which had the largest cumulative wake energy in all three years studied, has been eroding for many years (Tyler, 2016a, 2016b) having lost about 40% of its above-water area in the last century (Stott and Davis, 2003). The US Army Corps of Engineers works to reduce the loss of Egmont Key through beach nourishment (Brutsch et al., 2019). However, the relative contribution of ship wakes to the erosion of Egmont Key remains uncertain as the general processes of wind-driven waves and tidal currents

might also be important erosive drivers (Styles et al., 2016).

Wake energy should be evaluated relative to that of wind-driven waves (Houser, 2010; Kelpšaite et al., 2009; Silinski et al., 2015), particularly storm-driven waves. Significant wave heights  $\sim 2$  m have been recorded near the middle of Tampa Bay (Gilbert et al., 2009), but the fetch varies significantly across the bay, creating spatial variability of the wave field that should be taken into account in future studies. Wind can also alter wake structure (Fang et al., 2011). Topographic factors should also be considered, such as the presence and type of vegetation (Leonard and Luther, 1995), protective breakwaters (Dean et al., 1997) like those already deployed on the western shore of the spoil islands in Hillsborough Bay, and bottom slope that can induce wake shoaling and breaking (Friedrichs, 1948; Stive and De Vriend, 1995). These factors can alter sediment resuspension and erosive impact of wakes on the shoreline (Rapaglia et al., 2015; Zaggia et al., 2017). Additional considerations may arise when  $D \approx h$ . A sustained field program of high frequency water level measurements at key points in the bay would help address the above issues, and provide further testing of (1). Such testing should be designed to delimit the parameter range (e.g., vessel sizes, speeds, channel widths and depths) over which (1) is accurate.

The empirical relation (1) employed here to estimate wake heights assumes the vessels are operating in open water at low Froude number. These were reasonable assumptions given the size of Tampa Bay and vessel speeds examined. However, there are documented accounts of strong ship wakes being generated in confined regions of the bay which may require a different approach. The empirical model used here does not represent the effects of a restricted waterway. Application of recently developed analytical and numerical methods (Bellafiore et al., 2018; David et al., 2017; Pethiyagoda, 2016; Tezdogan et al., 2018) might be useful in this context. Access channels in Hillsborough Bay that range from about 150 to 250 m across are likely to experience confinement effects, particularly when  $D \approx h$ , and warrant additional study. Similarly, wakes from vessels operating at higher Froude numbers need a different approach. This is particularly true for the Enforcement class which is likely a significant source of wake energy.

Many maritime regions struggle with the sometimes conflicting need to protect environmental resources while providing economic opportunity to a growing population (Schipper et al., 2017; Sekovski et al., 2012; Woo et al., 2018). One potential risk to near-shore ecology and unprotected structures are wakes generated by ships passing through nearby waterways. This risk increases with ship number, size, and speed. This study was one of the first to examine wakes from a large number of vessels operating in a coastal region, over a wide range of hull dimensions and types, and over an extended period of time. Given the wide availability of AIS data, the methods developed here are easily transferrable to other locations, though the circumstance of vessels moving through constricted waterways would likely need to be considered separately.

#### Declaration of competing interest

The authors declare that they have no known competing financial interests or personal relationships that could have appeared to influence the work reported in this paper.

#### Acknowledgments

This effort received partial support from the Southeast Coastal Ocean Observing Regional Association (Sub Award #IOOS.16(028)USF.ML.OBS.1), the Gulf of Mexico Coastal Ocean Observing System (Award #02-S160275), the Greater Tampa Bay Marine Advisory Council-PORTS, Inc. (Award #2500-1066-00) the Tampa Bay Estuary Program (PO#6911), and US Fish and Wildlife (F17AC00815). The AIS data were provided by Marine Cadastre (<https://marinecadastre.gov/ais/>). Undergraduate researcher Rebecca George assisted with the AIS analysis.

#### References

- Barrass, B., Derrett, C.D., 2011. *Ship Stability for Masters and Mates*. Elsevier.
- Bauer, B.O., Lorang, M.S., Sherman, D.J., 2002. Estimating boat-wake-induced levee erosion using sediment suspension measurements. *J. Waterw. Port, Coast. Ocean Eng.* 128, 152–162.
- Bellafiore, D., Zaggia, L., Broglia, R., Ferrarin, C., Barbariol, F., Zaghi, S., Lorenzetti, G., Manfe, G., De Pascali, F., Benetazzo, A., 2018. Modeling ship-induced waves in shallow water systems: the Venice experiment. *Ocean Eng.* 155, 227–239.
- Benzaquen, M., Darmon, A., Raphael, E., 2014. Wake pattern and wave resistance for anisotropic moving disturbances. *Phys. Fluids* 26, 092106.
- Berman, G.A., Naar, D.F., Hine, A.C., Brooks, G.R., Tebbens, S.F., Donahue, B.T., Wilson, R., 2005. Geologic structure and hydrodynamics of Egmont channel: an anomalous inlet at the mouth of Tampa bay, Florida. *J. Coast Res.* 21, 331–357.
- Bertram, V., Schneekluth, H., 1998. *Ship Design for Efficiency and Economy*. Elsevier.
- Bilkovic, D.M., Mitchell, M., Davis, J., Andrews, E., King, A., Mason, P., Herman, J., Tahvildari, N., Davis, J., 2017. Review of Boat Wake Wave Impacts on Shoreline Erosion and Potential Solutions for the Chesapeake Bay. STAC 17-002, Edgewater, MD.
- Botha, C., 2000. Cathodic protection for ships. *Marine Technology* 31–35. May.
- Brutsch, K.E., Maglio, C.K., Tyler, Z.J., Ousley, J.D., Wang, P., 2019. Beneficial Use of Dredged Material with Increased Fine Sediment Content: A Case Study at Egmont Key, Florida. ERDC, Vicksburg, United States.
- Calil, J., Beck, M.W., Gleason, M., Merrifield, M., Klausmeyer, K., Newkirk, S., 2015. Aligning natural resource conservation and flood hazard mitigation in California. *PloS One* 10, e0132651.
- Chung, M.G., Dietz, T., Liu, J., 2018. Global relationships between biodiversity and nature-based tourism in protected areas. *Ecosystem Services* 34, 11–23.
- David, C.G., Roeber, V., Goseberg, N., Schlurmann, T., 2017. Generation and propagation of ship-borne waves—Solutions from a Boussinesq-type model. *Coast Eng.* 127, 170–187.
- Dean, R.G., Chen, R., Browder, A.E., 1997. Full scale monitoring study of a submerged breakwater, Palm Beach, Florida, USA. *Coast Eng.* 29, 291–315.
- Dias, F., 2014. Ship waves and Kelvin. *J. Fluid Mech.* 746, 1–4.
- Dontis, E.E., Radabaugh, K.R., Chappel, A.R., Russo, C.E., Moyer, R.P., 2020. Carbon Storage Increases with Site Age as Created Salt Marshes Transition to Mangrove Forests in Tampa Bay, Florida (USA), 43. *Estuaries and Coasts*, pp. 1470–1488.
- Ertekin, R.C., Webster, W.C., Wehausen, J.V., 1986. Waves caused by a moving disturbance in a shallow channel of finite width. *J. Fluid Mech.* 169, 275–292.
- Evans, M.W., Hine, A.C., Belknap, D.F., Davis, R.A., 1985. Bedrock controls on barrier island development: west-central Florida coast. *Mar. Geol.* 63, 263–283.
- Fang, M.C., Yang, R.Y., Shugan, I.V., 2011. Kelvin ship wake in the wind waves field and on the finite sea depth. *J. Mech.* 27, 71–77.
- Fenical, S., Kolomiets, P., Kivva, S., Zheleznyak, M., 2007. Numerical modeling of passing vessel impacts on berthed vessels and shoreline, 2006. *Coast Eng.* 1234–1246. World Scientific.
- Friedrichs, K.O., 1948. Waves on a shallow sloping beach. *Commun. Pure Appl. Math.* 1, 109–134.
- Froude, W., 1877. Experiments upon the Effect Produced on the Wave-Making Resistance of Ships by Length of Parallel Middle Body. Institution of Naval Architects.
- Gabel, F., Lorenz, S., Stoll, S., 2017. Effects of ship-induced waves on aquatic ecosystems. *Sci. Total Environ.* 601, 926–939.
- Gilbert, S., Robbins, B.D., Luther III, M.E., R., L.R., 2009. Field Measurements of Bottom Stress Due to Wave Action and Tidal Velocities in Tampa Bay to Support Seagrass Restoration and Shoreline Protection. Marine Science Associates report to the Hillsborough County Environmental Protection Commission.
- Gittman, R.K., Popowich, A.M., Bruno, J.F., Peterson, C.H., 2014. Marshes with and without sills protect estuarine shorelines from erosion better than bulkheads during a Category 1 hurricane. *Ocean Coast Manag.* 102, 94–102.
- Goodwin, C.R., 1987. Tidal Flow, Circulation, and Flushing Changes Caused by Dredge and Fill in Tampa Bay, Florida. U. S. Geological Survey Water Supply. Paper p. 88.
- Göransson, G., Larson, M., Althage, J., 2014. Ship-generated waves and induced turbidity in the gota äl river in Sweden. *J. Waterw. Port, Coast. Ocean Eng.* 140, 04014004.
- Hager, W.H., Castro-Orgaz, O., 2016. William Froude and the Froude number. *J. Hydraul. Eng.* 143, 02516005.
- Havelock, T., 1914. The propagation of disturbances in dispersive media. Cambridge tracts in mathematics and mathematical physics 17.
- Havelock, T.H., 1908. The propagation of groups of waves in dispersive media, with application to waves on water produced by a travelling disturbance. *Proceedings of the Royal Society of London. Series A* 81, 398–430.
- Herbert, D., Astrom, E., Bersoza, A.C., Batzer, A., McGovern, P., Angelini, C., Wasman, S., Dix, N., Sheremet, A., 2018. Mitigating erosional effects induced by boat wakes with living shorelines. *Sustainability* 10, 436.
- Houser, C., 2010. Relative importance of vessel-generated and wind waves to salt marsh erosion in a restricted fetch environment. *J. Coast Res.* 26, 230–240.
- Hüsigin, A., Linke, T., Zimmermann, C., 2000. Effects from supercritical ship operation on inland canals. *J. Waterw. Port, Coast. Ocean Eng.* 126, 130–135.
- Kelpšaite, L., Parnell, K., Soomere, T., 2009. Energy pollution: the relative influence of wind-wave and vessel-wake energy in Tallinn Bay, the Baltic Sea. *J. Coast Res.* 56, 812–816.
- Kelvin, L., 1887. On ship waves. *Proc. Inst. Mech. Eng.* 38, 409–434.
- Kelvin, L., 1906. I. Deep sea ship-waves. *The London, Edinburgh, and Dublin Philosophical Magazine and Journal of Science* 11, 1–25.
- Kriebel, D.L., Seelig, W.N., 2005. An Empirical Model for Ship-Generated Waves, Ocean Waves Measurement and Analysis. 5th Int. Symposium Waves, p. 10.

- Larsson, L., Eliasson, R., Orych, M., 2014. In: Principles of Yacht Design, fourth ed. Adlard Coles Nautical, London.
- Lee, B.W., Lee, C., 2019. Equation for ship wave crests in the entire range of water depths. *Coast Eng.* 153, 103542.
- Leonard, L.A., Luther, M.E., 1995. Flow hydrodynamics in tidal marsh canopies. *Limnol. Oceanogr.* 40, 1474–1484.
- Lim, G.J., Cho, J., Bora, S., Biobaku, T., Parsaei, H., 2018. Models and computational algorithms for maritime risk analysis: a review. *Ann. Oper. Res.* 1–22.
- Macfarlane, G., Cox, G., 2007. An introduction to the development of rational criteria for assessing vessel wash within sheltered waterways. *J. Mar. Des. Op.* 3–13, 2007.
- MacFarlane, G.J., 2006. Correlation of prototype and model scale wave wake characteristics for vessels operating at low Froude numbers. *Transactions of RINA - International Journal of Maritime Engineering* 148, 103–118.
- Mao, L.-l., Chen, Y.-m., Li, X., 2020. Characterizing ship-induced hydrodynamics in a heavy shipping traffic waterway via intensified field measurements. *Water Science and Engineering* 13, 329338.
- McTaggart, K., Stredulinsky, D., 2004. Validation of Ship Motion Predictions with Sea Trials Data for a Naval Destroyer in Multidirectional Seas, 25th Symposium on Naval Hydrodynamics. St. Johns, Newfoundland.
- Menéndez, P., Losada, I.J., Beck, M.W., Torres-Ortega, S., Espejo, A., Narayan, S., Díaz-Simal, P., Lange, G.-M., 2018. Valuing the protection services of mangroves at national scale: the Philippines. *Ecosystem services* 34, 24–36.
- Meyers, S.D., Luther, M.E., Ringuet, S., Raulerson, G., Sherwood, E., Conrad, K., Basili, G., 2020. Characterizing vessel traffic using the AIS: a case study in Florida's largest estuary. *J. Waterw. Port. Coast. Ocean Eng.* 146, 05020005.
- Mortensen, S.B., Alley, C., Kirkegaard, J., Hancock, R., 2009. Numerical modelling of moored vessel motions caused by passing vessels. *Coasts and Ports 2009: In a Dynamic Environment* 553–564.
- Neuman, D.G., Tapio, E., Haggard, D., Laws, K.E., Bland, R.W., 2001. Observation of long waves generated by ferries. *Can. J. Rem. Sens.* 27, 361–370.
- NOAA, 2015. Guidance for Considering the Use of Living Shorelines. NOAA, Silver Spring, Maryland.
- Noblesse, F., Zhang, C., He, J., Zhu, Y., Yang, C., Li, W., 2016. Observations and computations of narrow Kelvin ship wakes. *J. Ocean Eng. Sci.* 1, 52–65.
- Otvos, E.G., 1981. Barrier Island formation through nearshore aggradation — stratigraphic and field evidence. *Mar. Geol.* 43, 195–243.
- Papanikolaou, A., 2014. Ship Design: Methodologies of Preliminary Design. Springer.
- Parnell, K.E., Kofoed-Hansen, H., 2001. Waves from large high-speed ferries in confined coastal waters: management approaches with examples from New Zealand and Denmark. *Coast. Manag.* 29, 217–237.
- Parnell, K.E., Soomere, T., Zaggia, L., Rodin, A., Lorenzetti, G., Rapaglia, J., Scarpa, G.M., 2015. Ship-induced solitary riemann waves of depression in venice lagoon. *Phys. Lett.* 379, 555–559.
- Pethiyagoda, R., 2016. Mathematical and Computational Analysis of Kelvin Ship Wave Patterns. Queensland University of Technology.
- Pethiyagoda, R., McCue, S.W., Moroney, T.J., 2015. Wake angle for surface gravity waves on a finite depth fluid. *Phys. Fluids* 27, 061701.
- Pinkster, J., 2009. Suction, seiche, and wash effects of passing ships in ports. *Transactions-The Society of Naval Architects and Marine Engineers* 117, 99.
- Pranty, B., 2003. The Important Bird Areas of Florida: 2000–2002. Unpublished draft supplied by Audubon of Florida 444.
- Rabaud, M., Moisy, F., 2013. Ship wakes: Kelvin or mach angle? *Phys. Rev. Lett.* 110, 214503.
- Rapaglia, J., Zaggia, L., Parnell, K., Lorenzetti, G., Vafeidis, A.T., 2015. Ship-wake induced sediment remobilization: effects and proposed management strategies for the Venice Lagoon. *Ocean Coast Manag.* 110, 1–11.
- Rawson, K.J., Tupper, E.C., 2001. Basic Ship Theory. Elsevier.
- Rayleigh, L., 1885. On waves propagated along the plane surface of an elastic solid. *Proc. Lond. Math. Soc.* 1, 4–11.
- Safty, H.E., Marsooli, R., 2020. Ship wakes and their potential impacts on salt marshes in Jamaica bay, New York. *J. Mar. Sci. Eng.* 8, 325.
- Schipper, C., Vreugdenhil, H., De Jong, M., 2017. A sustainability assessment of ports and port-city plans: comparing ambitions with achievements. *Transport. Res. Transport Environ.* 57, 84–111.
- Schoellhamer, D.H., 1996. Anthropogenic sediment resuspension mechanisms in a shallow microtidal estuary. *Estuar. Coast Shelf Sci.* 43, 533–548.
- Scully, B., MacCartney, A., 2017. Use of AIS and AISAP for Analysis of Vessel Wakes in Charleston Harbor: A Case Study. ERDC/CHL CHETN-IX-46. Army Corps of Engineers, p. 11.
- Scully, B.M., 2016. Multi-Port Comparison of the Tidal Influence on Navigating Vessel Populations, Ports 2016. American Society of Civil Engineers, New Orleans, LA, pp. 832–842.
- Scully, B.M., Young, D.L., Ross, J.E., 2020. Mining marine vessel AIS data to inform coastal structure management. *J. Waterw. Port. Coast. Ocean Eng.* 146, 04019042.
- Sekovski, I., Newton, A., Dennison, W.C., 2012. Megacities in the coastal zone: using a driver-pressure-state-impact-response framework to address complex environmental problems. *Estuar. Coast Shelf Sci.* 96, 48–59.
- Silinski, A., Heuner, M., Schoelynck, J., Puijalon, S., Schröder, U., Fuchs, E., Troch, P., Bouma, T.J., Meire, P., Temmerman, S., 2015. Effects of wind waves versus ship waves on tidal marsh plants: a flume study on different life stages of *Scirpus maritimus*. *PloS One* 10, e0118687.
- Soares, C.G., 1993. Long term distribution of non-linear wave induced vertical bending moments. *Mar. Struct.* 6, 475–483.
- Soomere, T., 2006. Nonlinear ship wake waves as a model of rogue waves and a source of danger to the coastal environment: a review. *Oceanologia* 48, 185–202.
- Soomere, T., 2007. Nonlinear components of ship wake waves. *Appl. Mech. Rev.* 60, 120–138.
- Sorensen, R.M., Weggel, J.R., 1985. Development of ship wave design information. *Coastal Engineering* 1984 3227–3243.
- Sprandl, G.L., Gore, J.A., Cobb, D.T., 2000. Distribution of wintering shorebirds in coastal Florida. *J. Field Ornithol.* 71, 708–720.
- Stive, M.J., De Vriend, H.J., 1995. Shear stresses and mean flow in shoaling and breaking waves. *Coastal Engineering* 594–608, 1994.
- Stott, J.K., Davis Jr., R.A., 2003. Geologic development and morphodynamics of Egmont key, Florida. *Mar. Geol.* 200, 61–76.
- Styles, R., Brown, M., Brutsché, K., Li, H., Beck, T., Sánchez, A., 2016. Long-term morphological modeling of barrier island tidal inlets. *J. Mar. Sci. Eng.* 4, 65.
- Svanberg, M., Santén, V., Hörtborn, A., Holm, H., Finnsgård, C., 2019. AIS in maritime research. *Mar. Pol.* 103520.
- Tanimoto, K., Kobayashi, H., Ca, V.T., 2001. Ship waves in a shallow and narrow channel. *Coastal Engineering* 1141–1154, 2000.
- Teixeira, A., Soares, C.G., 2002. Assessment of Partial Safety Factors for Tankers, JCSS Workshop on Reliability Based Code Calibration, pp. 1–15.
- Tezdogan, T., Terziev, M., Oguz, E., Incecik, A., 2018. Numerical analysis of the behaviour of vessels advancing through restricted shallow waters. In: 3rd International Symposium on Naval Architecture and Maritime.
- Toby, A.S., 1997. US high speed destroyers, 1919–1942: hull proportions. *Nav. Eng. J.* 109, 155–177.
- Tu, E., Zhang, G., Rachmawati, L., Rajabally, E., Huang, G.-B., 2018. Exploiting AIS data for intelligent maritime navigation: a comprehensive survey from data to methodology. *IEEE Trans. Intell. Transport. Syst.* 19, 1559–1582.
- Tyler, Z.J., 2016a. Morphodynamics of Egmont Key at the Mouth of Tampa Bay. West-Central Florida. University of South Florida, M.S. Thesis.
- Tyler, Z.J., 2016b. Morphodynamics of Egmont Key at the Mouth of Tampa Bay: West-Central Florida. University of South Florida.
- Vincent, M.S., 2001. Development, Implementation and Analysis of the Tampa Bay Coastal Prediction System, p. 252. Department of Civil and Environmental Engineering. College of Engineering, University of South Florida, Tampa, FL.
- Watson, D.G., 2002. Practical Ship Design. Elsevier.
- Weggel, J.R., Sorensen, R.M., 1986. Ship Wave Prediction for Port and Channel Design, Ports, vol. 86. ASCE, pp. 797–814.
- Westerdijk, L., Beekveld, M., Eiben, A., Belitser, E., 2019. Classifying Vessel Types Based on AIS Data, p. 80. Vrije Universiteit Amsterdam.
- Woo, J.-K., Moon, D.S., Lam, J.S.L., 2018. The impact of environmental policy on ports and the associated economic opportunities. *Transport. Res. Pol. Pract.* 110, 234–242.
- Yousefi, R., Shahaghian, R., Shakeri, M., 2013. Hydrodynamic analysis techniques for high-speed planing hulls. *Appl. Ocean Res.* 42, 105–113.
- Zaggia, L., Lorenzetti, G., Manfè, G., Scarpa, G.M., Molinaroli, E., Parnell, K.E., Rapaglia, J.P., Gionta, M., Soomere, T., 2017. Fast shoreline erosion induced by ship wakes in a coastal lagoon: field evidence and remote sensing analysis. *PloS One* 12, e0187210.
- Zhang, P., Zhu, D.-x., Leng, W.-h., 2008. Parametric approach to design of hull forms. *Journal of Hydrodynamics, Ser. B* 20, 804–810.
- Zhou, Y., Daamen, W., Vellinga, T., Hoogendoorn, S., 2019. Review of maritime traffic models from vessel behavior modeling perspective. *Transport. Res. C Emerg. Technol.* 105, 323–345.
- Zhu, Y., He, J., Wu, H., Li, W., Noblesse, F., 2018. Basic models of farfield ship waves in shallow water. *J. Ocean Eng. Sci.* 3, 109–126.
- Zhu, Y., He, J., Zhang, C., Wu, H., Wan, D., Zhu, R., Noblesse, F., 2015. Farfield waves created by a monohull ship in shallow water. *Eur. J. Mech. B Fluid* 49, 226–234.